Commun. Comput. Phys.
doi: 10.4208/cicp.2009.09.099

Vol. 7, No. 4, pp. 674-682
April 2010

Simultaneous Prediction of Morphologies of a Critical Nucleus and an Equilibrium Precipitate in Solids

Lei Zhang[1], Long-Qing Chen[2] and Qiang Du[1,2,*]

[1] *Department of Mathematics, Penn State University, PA 16802, USA.*
[2] *Department of Materials Science and Engineering, Penn State University, PA 16802, USA.*

Received 11 June 2009; Accepted (in revised version) 4 September 2009

Communicated by Jie Shen

Available online 12 October 2009

Abstract. We investigate the critical nucleus and equilibrium morphologies during precipitation of a second-phase particle in a solid. We show that a combination of diffuse-interface description and a constrained string method is able to predict both the critical nucleus and equilibrium precipitate morphologies simultaneously without *a priori* assumptions. Using the cubic to cubic transformation as an example, it is demonstrated that the maximum composition within a critical nucleus can be either higher or lower than that of equilibrium precipitate while the morphology of an equilibrium precipitate may exhibit lower symmetry than the critical nucleus resulted from elastic interactions.

AMS subject classifications: 74G15, 74B20

Key words: Phase field, diffuse interface, nucleation, critical nucleus, constrained string method, elasticity.

1 Introduction

Precipitation is a common, natural process which takes place in a supersaturated solid or liquid solution, e.g., during isothermal annealing of a quenched homogeneous alloy within a two-phase field of a phase diagram. It is the basic process that underlies the development of many advanced materials such as high-temperature superalloys and ultralight aluminum and magnesium alloys. The precipitate microstructure (the number density, volume fraction, and morphology) is the dominant factor that determines

*Corresponding author. *Email addresses:* zhang_l@math.psu.edu (L. Zhang), lqc3@psu.edu (L.-Q. Chen), qdu@math.psu.edu (Q. Du)

the mechanical properties of a solid. One of the main challenges in predicting precipitate microstructures in solids has been the determination of precipitate particle morphology because of the presence of both interfacial energy anisotropy and anisotropic elastic interactions. As the majority of precipitation reactions in solids take place through a nucleation-and-growth mechanism followed by particle coarsening, there are two thermodynamically well-defined morphologies: the morphology of a critical nucleus and the equilibrium morphology of a precipitate particle.

In classical nucleation models, a critical nucleus is usually assumed to be spherical and critical radius is determined by a competition between a bulk free energy decrease which is proportional to volume and an interfacial energy increase which is proportional to interfacial area. In a diffuse-interface description, a critical nucleus is defined as the composition or order parameter fluctuation having the minimum free energy increase among all fluctuations which lead to nucleation, i.e., the saddle point configuration along the minimum energy path (MEP) between the metastable initial phase represented by a local minimum in the free energy landscape and the equilibrium phase represented by the global minimum. Therefore, nucleation of new precipitate particles requires overcoming a thermodynamic barrier. The magnitude of the nucleation barrier, and thus the nucleation rate, or the resulted precipitate particle density, is strongly dependent on the morphology of critical nuclei. On the other hand, following nucleation and growth, the morphology and volume fraction of precipitate particles during coarsening are generally close to equilibrium. The particle morphology and volume fraction during coarsening together with the particle density predicted from nucleation provide all the information that is needed for predicting the strength of a solid in mechanistic models.

There have been extensive studies, particularly numerical simulations, of equilibrium shapes of a precipitate particle in solids using both sharp- and diffuse-interface approaches [5, 7, 8, 11–13]. Attempts have also been made to predict the morphology of a critical nucleus in solids by taking into account both interfacial energy anisotropy and anisotropic elastic interactions [9, 10, 14–16]. For example, we showed that one can predict the morphology of a critical nucleus in a system going through a phase transition [14–16] using a combination of the diffuse-interface (phase-field) description and the minimax algorithm based on the mountain pass theorem. The main objective of this letter is to report a first attempt to predict the morphology of a critical nucleus as well as the equilibrium morphology of a precipitate simultaneously within the same physical model and mathematical formulation. A concentration field that conserves the average concentration is considered as an illustration. We extend the string method [3, 4] to systems with constraints through a novel augmented Lagrange multiplier formulation. This leads to an effective constrained string method which may be useful in the study of many constrained barrier crossing problems in physics, chemistry and biology. In this work, we demonstrate that a combination of diffuse-interface description and the constrained string method can simultaneously predict the morphologies of a critical nucleus and an equilibrium precipitate which can be dramatically different.

2 Diffuse interface model

Following the diffuse-interface theory of Cahn-Hilliard [1], we consider a conserved field c which describes the concentration distribution in a binary solid. The change of the total free energy, F_t, arising from the compositional fluctuation in an initially homogeneous state with c_0 is given by

$$F_t(c) = \int_\Omega \left(\frac{1}{2}|A\nabla c|^2 + \delta f(c) \right) d\mathbf{x} + \beta E_e(c). \tag{2.1}$$

We use the domain $\Omega = (-1,1)^d$ with d being the space dimension. A periodic boundary condition is used for c with the period sufficiently large in comparison with the size of the nucleus and the equilibrium particle so the effect of boundary conditions is negligible. The gradient energy coefficient A is a constant diagonal tensor for isotropic interfacial energy, while for anisotropic interfacial energy, it can be made to be either directionally dependent or dependent on the derivatives of c. In [14], the effect of anisotropic interfacial energy on the critical nuclei morphology has been examined in the case of a non-conserved field. In this work, we choose to focus on the case of isotropic interfacial energy with A being a constant multiple of the identity tensor. The local free energy density change $\delta f(c)$, arising from a compositional fluctuation around the homogeneous state with composition c_0, is given by

$$\delta f(c) = \frac{1}{4\kappa}[(c^2-1)^2 - (c_0^2-1)^2 - 4(c-c_0)(c_0^3-c_0)],$$

where κ is a coefficient of energy density. The plots of $\delta f = \delta f(c)$ are given in Fig. 1 for different c_0 at $\kappa = 0.03$, with $c_s = -\sqrt{3}/3$ being the spinodal composition.

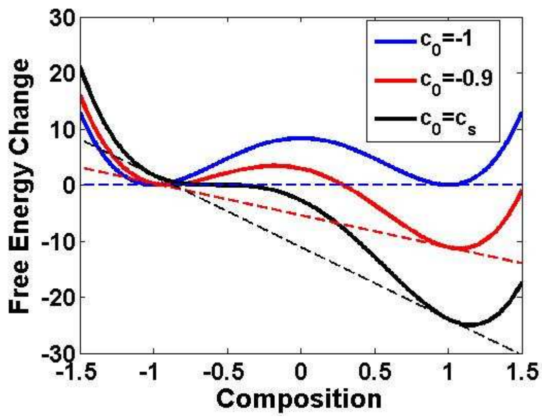

Figure 1: Free energy change for $c_0 = -1$, -0.9 and c_s.

Assuming that the elastic modulus is anisotropic but homogeneous, the microscopic elasticity theory of Khachaturyan [6] can be conveniently employed to efficiently calculate the elastic strain energy for simply connected coherent inclusions in a solid. For the case of cubic precipitates in a cubic matrix, the elastic energy contribution can be written as

$$E_e(c)=\frac{1}{2(2\pi)^d}\int_{\hat{\Omega}} d\mathbf{k} B(\mathbf{n})|\hat{c}(\mathbf{k})-\hat{c}_0(\mathbf{k})|^2. \tag{2.2}$$

$\hat{c}(\mathbf{k})$ is the Fourier transform of $c(\mathbf{x})$. The integration in (2.2) is over the reciprocal space $\hat{\Omega}$ of the reciprocal lattice vector $\mathbf{k}$, $\mathbf{n}=\mathbf{k}/|\mathbf{k}|=(n_1, n_2, n_3)$ is the normalized unit vector and $B(\mathbf{n})$ is given by [6]

$$B(\mathbf{n})=3(c_{11}+2c_{12})\epsilon_0^2-\frac{(c_{11}+2c_{12})^2\epsilon_0^2(1+2\zeta s(\mathbf{n})+3\zeta^2 n_1^2n_2^2n_3^2)}{c_{11}+\zeta(c_{11}+c_{12})s(\mathbf{n})+\zeta^2(c_{11}+2c_{12}+c_{44})n_1^2n_2^2n_3^2}, \tag{2.3}$$

where $\zeta=(c_{11}-c_{12}-2c_{44})/c_{44}$ is the elastic anisotropic factor with c_{11}, c_{12}, c_{44} being elastic constants in the Voigt's notation, ϵ_0 is the lattice mismatch between the new nucleating cubic phase and the parent cubic phase, and $s(\mathbf{n})=n_1^2n_2^2+n_1^2n_3^2+n_2^2n_3^2$. We set, in particular that, $\mathbf{n}=0$ if $\mathbf{k}=0$.

Rather than varying the magnitude of lattice mismatch and elastic constants, a factor β is introduced in (2.1) to study the effect of relative elastic energy contribution to chemical driving force on the critical nucleus morphology and equilibrium particle morphology.

For a conserved field with profile $c=c(x)$, the computation of saddle points and the minimum energy path for the energy functional (2.1) subject to the constraint

$$\int_{\Omega}(c(x)-c_0)dx=0. \tag{2.4}$$

is carried out via the constrained string method which is a natural extension of the simplified string method originally developed by E, Ren and Vanden-Eijnden [3,4]. We outline the algorithmic procedures here. Some related mathematical theory can be found in [2] while detailed numerical analysis will be given elsewhere.

The string methods proceed by evolving a string, i.e., a smooth curve with intrinsic parametrization, to the MEP between two metastable/stable regions in configuration space. Specifically, let $\varphi(\alpha,t)$ denote the instantaneous position (representing the composition profile in our case) of the string with α being a suitable parametrization. For an energy $E=E(\varphi)$, the evolution of the string is based on first taking a gradient decent direction via the dynamic equation

$$\varphi_t=-\frac{\delta E}{\delta\varphi}(\varphi),$$

then followed by a projection step that maps φ back to a configuration satisfying the specified parametrization [4]. Here, $\frac{\delta E}{\delta\varphi}$ represents the variational derivative of the energy E with respect to φ. In practice, a commonly used parametrization for a string discretized by a finite number of line segments is to enforce an equal segment length condition through an interpolation procedure [4]. Sufficient number of segments are needed to ensure both the convergence and the accuracy of the algorithm. Based on such an idea, we developed a constrained string method to find the MEP on general constrained manifolds. It follows essentially the string method with additional treatment of the constraints.

The constrained string method allows several equivalent formulations such as the penalty or Lagrange multiplier methods. Yet, some formulations are more natural and robust than others and require less parameter tuning. One particularly effective approach is based on the augmented Lagrange multiplier method. Its application to the energy (2.1), subject to the simple constraint (2.4), amounts to consider a modified total energy involving two parameters λ and M:

$$E_\lambda(\varphi)=F_t(\varphi)+\lambda\int_\Omega(\varphi-c_0)dx+M\Big(\int_\Omega(\varphi-c_0)dx\Big)^2.$$

For a fixed positive penalty constant M, we solve for the constrained string, via the following iterations: first, given λ_j, we apply the string method [4] to the modified energy E_{λ_j}=$E_{\lambda_j}(\varphi)$ to solve for φ_j; then, with φ_j known, we update λ_j by λ_{j+1} via:

$$\lambda_{j+1}=\lambda_j+2M\int_\Omega(\varphi_j-c_0)dx.$$

We iterate between these two steps until convergence. At the end of iteration, the constrained MEP is found with the equation (2.4) satisfied along the string, and the limit of λ_j gives the corresponding Lagrange multiplier. Adopting this formulation, the implementation of the constrained string method is straightforward and it assures the satisfaction of the constraint without requiring M to be exceedingly large, thus reducing the stiffness of the dynamic system. The constrained string method including the augmented Lagrange multiplier formulation can be derived for very general energies and constrained manifolds and thus have many potential applications. For the case of the energy functional F_t, each point of the string corresponds to a composition profile along the MEP. The critical nucleus is determined by the composition profile c=$c(x)$ which is recovered from the saddle point corresponding to the point on the converged MEP with the highest energy.

3 Numerical simulations

The model and algorithm described above allows us to determine both the critical nucleus and equilibrium precipitate. As an illustration, we focus on the two-dimensional example of a cubic to cubic transformation. We fix one end of the string to be the initial state representing a uniform composition with $c(x)=c_0$ in Ω, while allowing the other end to move but generally within the energy well of the ground state or equilibrium solution. We use 31 points (30 line segments) to discretize the string and the Fourier spectral method with a 256×256 grid for computing each composition profile, i.e., point on the

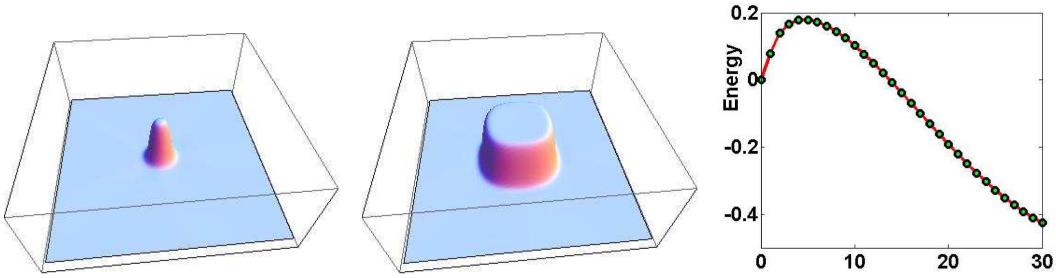

Figure 2: Critical nucleus, equilibrium and MEP for c_0=-0.9.

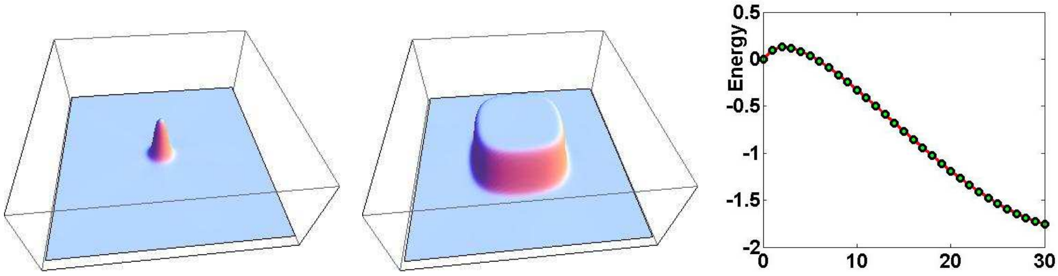

Figure 3: Critical nucleus, equilibrium and MEP for c_0=-0.88.

string. An adaptive rescaling of the computational domain along the string can be used to further improve the resolution. Numerical tests were conducted to ensure that sufficient resolution can be achieved. We fix the parameters A_1=A_2=1.56×10^{-4}, c_{11}=250, c_{12}=150, c_{44}=200 and ϵ_0=0.02. Since both critical nucleus and equilibrium solution are relatively small in comparison to the spatial domain Ω, their plots are magnified by a factor of 2 in order to get a better view.

In Fig. 2, for κ=0.7 and β=0.5, we plot the critical nucleus (left) and equilibrium solution (center) and the MEP (right) in the presence of the long-range elastic interactions corresponding to an average composition c_0=-0.9. One of the interesting observations is that the maximum composition within the critical nucleus is about 5% higher than that of the equilibrium precipitate. For this c_0, however, both the critical nucleus and equilibrium precipitate have the same cubic symmetry due to the elastic energy interactions.

Another example is shown in Fig. 3 when c_0 is changed to -0.88. As c_0 is close to the spinodal point, the interface of critical nucleus becomes more diffusive. The composition value at the center of a critical nucleus decreases and is about 5% smaller than the composition of the equilibrium precipitate. Moreover, the size of the equilibrium precipitate is larger for c_0=-0.88 than for c_0=-0.9 as a result of higher supersaturation.

In both Figs. 2 and 3, the MEP plots reveal how the energy values change from the initial state to the final equilibrium state along points on the string (corresponding to total 31 different composition profiles). The value of critical energy needed to nucleate a new particle for c_0=-0.88 is 0.1282 which is significantly lower than the value of 0.1792 for c_0=-0.9.

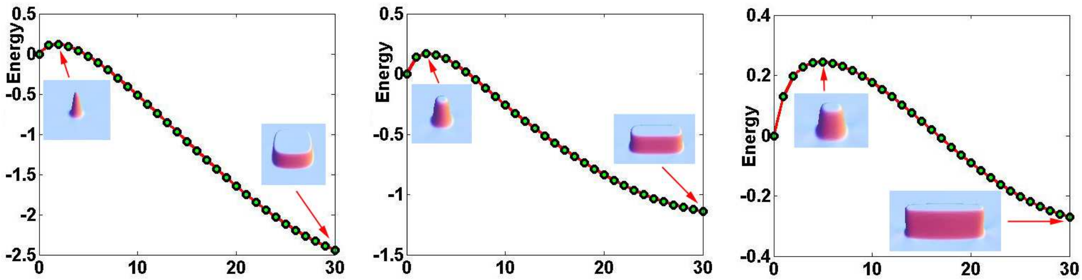

Figure 4: Calculated MEPs for β=0.5, 1 and 1.5 with inserts showing the critical nuclei and equilibria.

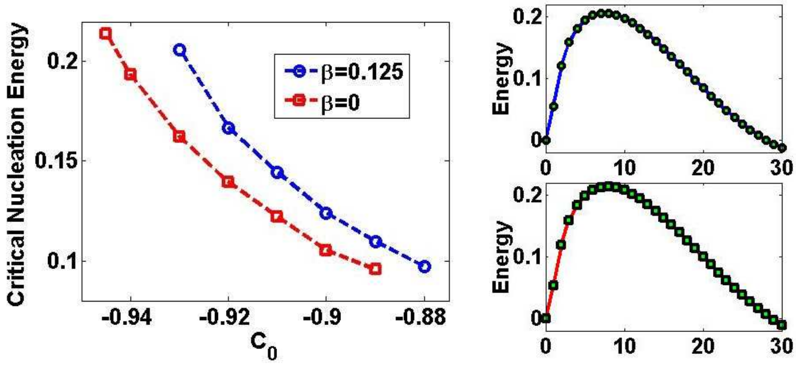

Figure 5: Critical nucleation energy with changing c_0 for β=0.125 and 0 (left) and MEPs (right) for c_0=-0.93, β=0.125 and c_0=-0.945, β=0.

To examine the effect of elastic energy contributions, we fix the chemical driving force with $c_0=-0.85$ and $\kappa=1$, and increase β to compute the MEPs. In Fig. 4 (left), we plot the MEPs (with the compositional profiles for the critical nucleus and equilibrium precipitate as inserts) for different values of β. At a relatively small elastic energy contribution, both the critical nucleus and the equilibrium precipitate display a cubic symmetry. With higher elastic strain energy contribution, while the critical nucleus maintains the cubic symmetry, the equilibrium precipitate is plate-like with only two-fold symmetry (Fig. 4, center). As we further increase the elastic energy contribution, for example, $\beta=1.5$, both the critical nucleus and the equilibrium precipitate exhibit plate-shaped particles (Fig. 4, right). We also observe the increases in both the critical nucleus size (see the inserts) and the nucleation energy barrier (from 0.1222 to 0.1708 and 0.2449) with increasing elastic energy contributions.

The influence of elastic energy contributions on the morphologies of both critical nuclei and equilibrium precipitates can be understood from the competition between interfacial energy and elastic strain energy. The total interfacial energy is proportional to interfacial area between a particle and the matrix while the total elastic strain energy is proportional to the volume of the particle. Since the size of a critical nucleus is significantly smaller than that of an equilibrium precipitate, it is expected that the elastic energy will have a lesser influence on the critical nucleus (assuming the interfacial coherency between the particle and matrix is always maintained during the entire evolution process). Minimization of elastic strain energy leads to plate-shaped particles while minimization of interfacial energy (assuming isotropic) leads to spherical shapes. Therefore, as the elastic strain energy contribution increases, the shape of the equilibrium precipitate bifurcates first from being cubic to plate-shaped before the critical nucleus does.

To further understand the elastic energy contributions,in Fig. 5 (left), the critical free energy of formation as a function of average composition c_0 is plotted for the case without the elasticity contribution β=0 (red squares), and for critical nuclei with β=0.125 (blue circles). We take $\kappa=1$ in both cases. As expected, with the increase of the average composition, the size of critical nuclei (with cubic symmetry) is reduced and the critical nucleation energy decreases. This dependence is similar to that predicted from the classical nucleation theory for spherical particles. We also notice that, for the given parameters and elastic energy, the smallest c_0 which allows nucleation to happen is -0.93, where the energy of equilibrium solution is very close to the initial-state energy (Fig. 5, top right). If c_0 is smaller than -0.93, the energy of an equilibrium precipitate becomes higher than the initial homogeneous state, indicating that the initial uniform state could be globally stable so that the elastic energy contribution can prevent the nucleation process from occurring, i.e. coherency strain energy contribution shifts the equilibrium phase boundary. Without elasticity, nucleation can still take place with an even smaller c_0=-0.945 (Fig. 5, bottom right).

4 Summary

In summary, we report a new approach for computing the morphologies of both critical nuclei and equilibrium precipitates without *a priori* shape assumptions. Our calculations reveal that the morphology of a critical nucleus can be dramatically different from the equilibrium one due to the elastic energy contributions. We plan to extend the approach to treat systems with defects such as dislocations and interfaces, i.e., processes of heterogeneous nucleation. Moreover, while the focus of this letter is on the precipitate nucleation and the equilibrium state, the mathematical and computational framework can be potentially applied to other constrained barrier crossing problems in physics, chemistry and biology, including examples like the saddle point search for activated states in solid state diffusion using density function theory, and the determination of domain morphology of a critical nucleus and a switched state in ferroelectric solids under an applied electric field.

Acknowledgments

This research is supported in part by NSF-DMS 0712744, NSF DMR-0710483 and NSF-IIP 541674 Center for Computational Materials Design (CCMD).

References

[1] J. Cahn and J. Hilliard, Free energy of a nonuniform system. III. Nucleation in a two-component incompressible fluid, J. Chem. Phys., 31 (1959), pp.688-699.

[2] Q. Du and L. Zhang, A constrained string method and its numerical analysis, to appear in Comm. Math. Sci., 2009.

[3] W. E, W. Ren and E Vanden-Eijnden, String method for the study of rare events, Phys. Rev. B, 66, 052301, (2002).

[4] W. E, W. Ren and E Vanden-Eijnden, Simplified and improved string method for computing the minimum energy paths in barrier-crossing events, J. Chem. Phys., 126, 164103, 2007.

[5] H.J. Jou, P.H. Leo and J.S. Lowengrub, Microstructural Evolution in Inhomogeneous Elastic Media, J. Comp. Phys., 131 (1997), pp.109-148.

[6] A.G. Khachaturyan, Theory of Structural Transformations in Solids, Wiley, New York, (1983).

[7] J.K. Lee, Morphology of coherent precipitates via a discrete atom method, Mat. Sci. Eng. A, 238 (1997), pp.1-12.

[8] R. Mueller and D. Gross, 3D simulation of equilibrium morphologies of precipitates, Comp. Mat. Sci., 11 (1998), pp.35-44.

[9] A. Roy, J.M. Rickman, J.D. Gunton and K.R. Elder, Simulation study of nucleation in a phase-field model with nonlocal interactions, Phys. Rev. E, 57 (1998), pp.2610-2617.

[10] C. Shen, J.P. Simmons and Y. Wang, Effect of elastic interaction on nucleation: I. Calculation of the strain energy of nucleus formation in an elastically anisotropic crystal of arbitrary microstructure, Acta Materialia, 54 (2006), pp.5617-5630.

[11] M.E. Thompson and P.W. Voorhees, Equilibrium particle morphologies in elastically stressed coherent solids, Acta Materialia, 47 (1999), pp.983-996.

[12] Y. Wang, L.Q. Chen and A.G. Khachaturyan, Kinetics of strain-induced morphological transformation in cubic alloys with a miscibility gap, Acta Materialia, 41 (1993), pp.279-296.

[13] C. Wolverton, First-principles prediction of equilibrium precipitate shapes in Al-Cu alloys, Phil. Mag. Lett., 79 (1999), pp.683-690.

[14] L. Zhang, L.Q. Chen and Q. Du, Morphology of critical nuclei in solid state phase transformations, Phys. Rev. Lett., 98, 265703 (2007)

[15] L. Zhang, L.Q. Chen and Q. Du, Diffuse-interface description of strain-dominated morphology of critical nuclei in phase transformations, Acta Materialia, 56 (2008), pp.3568-3576.

[16] L. Zhang, L.Q. Chen and Q. Du, Mathematical and Numerical Aspects of Phase-field Approach to Critical Morphology in Solids, J. Sci. Comput., 37 (2008), pp.89-102.